

Original research article

Experiment demonstration of DFB semiconductor laser array based on S-bent waveguide with sampled grating



Xuemei Liang^a, Xing Zhang^{b,*}, Yong-Yi Chen^{b,c,*}, Yun-shan Zhang^{d,**}

^a College of Information Technology, Jilin Agricultural University, Changchun 130118, China

^b State Key Laboratory of Luminescence and Application, Changchun Institute of Optics, Fine Mechanics and Physics, Chinese Academy of Sciences, Changchun 130033, China

^c Peng Cheng Laboratory, No.2, Xingke 1st Street, Nanshan, Shenzhen, China

^d College of Electronic and Optical Engineering & College of Microelectronics, Nanjing University of Posts and Telecommunications, Nanjing, 210023, China

ARTICLE INFO

Keywords:

Laser array
Bragg grating
Semiconductor laser
Multiwavelength

ABSTRACT

A four-wavelength DFB laser array based on S-bent waveguide and sampled grating is experimentally demonstrated. The laser array shows good single mode operation and uniform wavelength spacing. Since the fabrication for multi-wavelength of the gratings only requires conventional sampled grating combined with s-bent waveguides, the whole laser chip fabrication is very simple.

1. Introduction

Multiwavelength DFB laser array (MLA) is one of the key elements in the Wavelength Division Multiplexing (WDM) communication systems and the monolithic integrated circuits [1–3]. In these applications, the lasing wavelength should be precisely matched to the ITU-T standard, and single mode operation must be ensured for each laser in the same array chip. These two key issues require accurate fabrication for the Bragg grating [4,5]. For example, the 0.8 nm wavelength spacing requires the grating period difference of ~ 0.13 nm and the grating phase change should be inserted for the single mode operation. The nanometer fine structure grating [6–13] is a big challenge especially for large scale fabrication. Up to now, the mostly used method is the e-beam lithography [1,14,15]. But it writes gratings point by point resulting in tedious time consumption and high cost [16]. In former studies [17,18], we proposed a new method to realize the MLA, i.e., S-bent waveguide (SBW-DFB) with sampled grating. In such method [17,18], the uniform sampled grating is used for the multi-wavelengths' grid and the S-bent waveguide introduces a phase change in the grating to set up an effective single mode resonance. Furthermore, the sampling structure is in micrometer scale and the basic grating is uniform, which highly simplifies the fabrication process and can be realized by common holographic exposure and photolithography. We successfully demonstrated a single wavelength laser based on this method [19] experimentally. Good single mode operation has been achieved. In this paper, we further fabricated a four-wavelength array. Uniform wavelength spacing and high single mode operation have been experimentally demonstrated. These results show that the proposed method should be a promising way for the future MLA with low cost fabrication.

* Corresponding authors at: State Key Laboratory of Luminescence and Application, Changchun Institute of Optics, Fine Mechanics and Physics, Chinese Academy of Sciences, Changchun 130033, China.

** Corresponding author.

E-mail addresses: zhangx@ciomp.ac.cn (X. Zhang), chenyy@ciomp.ac.cn (Y.-Y. Chen), yszhang@njupt.edu.cn (Y.-s. Zhang).

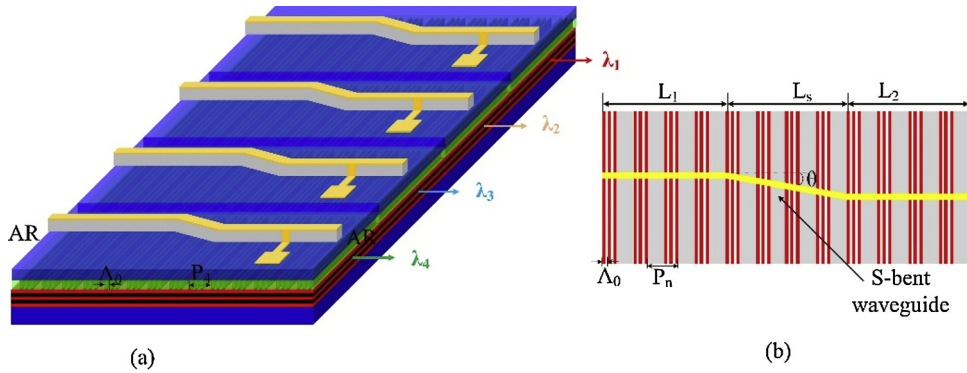


Fig. 1. schematic of the (a) 4-channel DFB laser arrays with s-bent waveguides and sampled gratings, (b) s-bent waveguide and sampled grating.

2. The laser structure and principle

The structures of the four-channel SBW-DFB laser arrays are shown in Fig. 1(a). The SBW-DFB lasers have the same semiconductor material as the conventional multiple-quantum-well (MQW) DFB laser. The gratings in the SBW-DFB lasers are uniform sampled gratings designed by the REC technique. The main difference between the conventional MQW DFB laser and the SBW-DFB laser is that, there is an s-bent waveguide in the center of the SBW-DFB laser.

According to the Fourier analysis, the sampled grating as shown in Fig. 1(b) can be expressed as [20]

$$\Delta n(z) = \frac{1}{2} \Delta n_s \sum_m F_m \exp \left[j \left(2\pi \frac{z}{\Lambda_0} + 2m\pi \frac{z}{P} \right) \right] + c. c \quad (1)$$

where P is the sampling period, Λ_0 is the period of the basic grating (seed grating), Δn_s is the index modulation of the seed grating, m denotes the m th order Fourier series and F_m is the Fourier coefficient of the m th subgrating. Usually the +1st order subgrating is used as the equivalent grating for DFB lasers, and the period of the +1st order subgrating Λ_{+1} can be expressed as

$$\Lambda_{+1} = \frac{\Lambda_0 P_n}{(P_n + \Lambda_0)} \quad (2)$$

Therefore, the lasing wavelength controlled by the +1st subgrating can be changed by sampling period P . The grating period in the bent waveguide region can be expressed as [17]

$$\Lambda_s = \frac{\Lambda_{+1}}{\cos \theta} = \frac{\Lambda_0 P_n}{(P_n + \Lambda_0) \cos \theta} \quad (3)$$

Here, θ is the tilted angle of the bent waveguide. It can be seen that Λ_s is larger than Λ_{+1} , and a continuous phase change in grating can be induced in the bent waveguide region, which is also called phase adjust region (PAR), i.e., corrugated pitch modulation (CPM). Through changing the tilted angle θ of the bent waveguide, various phase shifts in the PAR can be realized. According to Ref. [17], when a π phase shift is induced in the PAR, the relationship between Λ_s and Λ_{+1} should be expressed as follows:

$$\frac{L_s}{\Lambda_{+1}} - \frac{L_s}{\Lambda_s} = \frac{1}{2} \quad (4)$$

We have designed four-wavelength SBW-DFB lasers arrays with 3.2 nm wavelength spacing. The parameters of the two lasers are listed in Table 1. The total cavity length is 1000 μm and the length of the s-bent area (L_s) is 400 μm with two 300 μm -long straight waveguides (L_1 and L_2) on both sides. The tilted angle of the s-bent waveguide is 1.4°. The Bragg wavelength of the seed grating is set

Table 1
Parameters of the SBW-DFB laser arrays.

Parameters	No. 17	No. 18	No. 19	No.20
Total cavity length (μm)	1000	1000	1000	1000
L1 (μm)	300	300	300	300
Ls (μm)	400	400	400	400
L2 (μm)	300	300	300	300
Tilted angle θ	1.4°	1.4°	1.4°	1.4°
Seed grating period Λ_0 (nm)	256	256	256	256
Sampling period P (μm)	5095	5367	5648	5972
Effective refractive index (at 1550 nm)	3.2	3.2	3.2	3.2

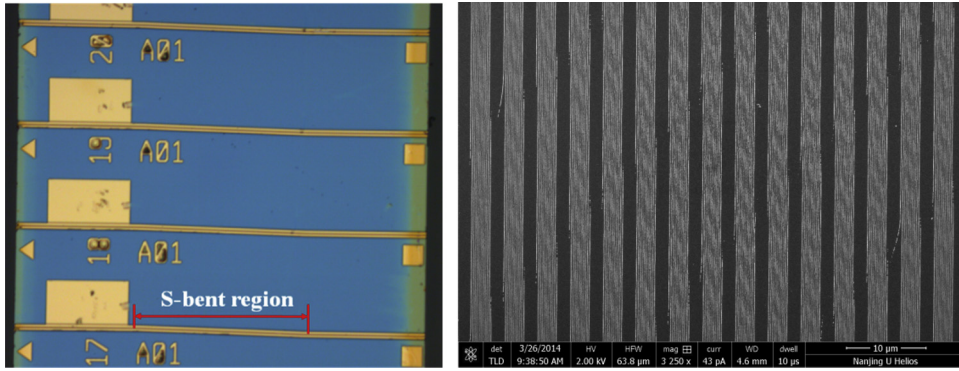


Fig. 2. (a) Fabricated devices of the 4-channel DFB laser arrays with s-bent waveguides under optical microscope; (b) SEM picture of sampled grating.

at 1642 nm, which is far away from the gain region and cannot lase. In order to obtain 3.2 nm wavelength spacing, the sampling periods of the four DFB lasers are set at 5.095 μm , 5.367 μm , 5.648 μm and 5.972 μm respectively.

3. Experiment results and discussion

The total wafer is grown by a conventional two-stage metal-organic chemical vapor deposition (MOCVD). The first epitaxial structure of our SBW-DFB includes an n-InP buffer layer, an n-InAlGaAs lower optical confinement layer, an InAlGaAs MQW structure, a p-InAlGaAs upper optical confinement layer and a 30 nm thick p-InAlGaAs grating layer placed on the n-InP substrate. Then, a conventional holographic exposure is carried out to make the seed grating, and followed by a conventional photolithography to realize the uniform sampled grating. The fabrication of the sampled grating is the same as the common method as shown in [21,22]. After fabricating the sampled grating, a p-InP cladding layer and a p-InGaAs contact layer are regrown over the entire wafer using second epitaxy using MOCVD. The following steps are common semiconductor fabrication steps, including processing s-bent ridge waveguides with conventional photolithography, SiO₂ deposition for insulation layer using plasma chemical vapor deposition

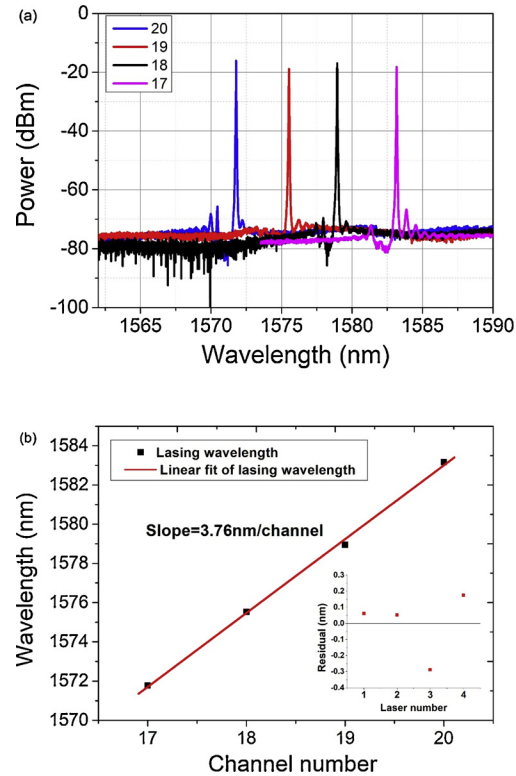


Fig. 3. (a) Measured spectrum characteristics of the SBW-DFB lasers' array. (b) Lasing wavelengths' distribution of the SBW-DFB lasers' array.

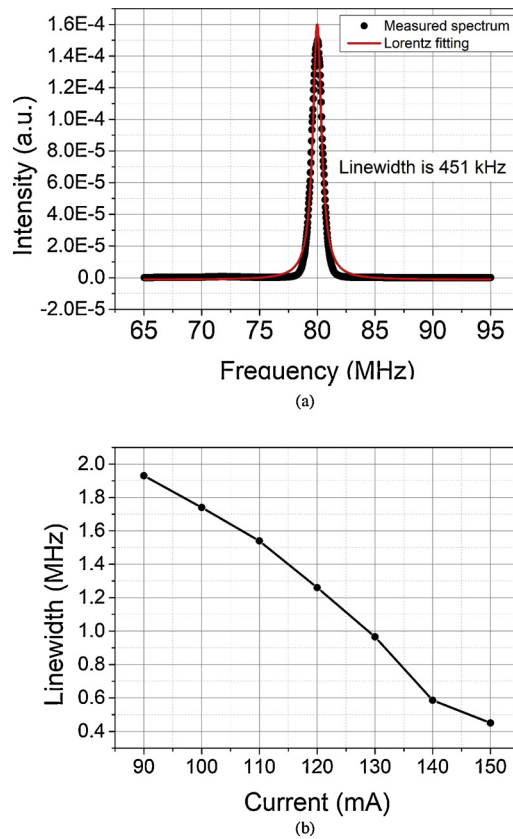


Fig. 4. (a) Measured linewidth characteristics for No. 20 of the SBW-DFB lasers' array at 25 °C and current is 150 mA. (b) Lasing linewidth versus the injection current. Maxium lasing linewidth is 1.93 MHz at 90 mA, and minimum linewidth is 451 kHz at 150 mA.

(PECVD), opening p-metal contact windows with photolithography and inductively coupled plasma (ICP) etching, making p-side ohmic contacts, wafer thickness reduction and making n-side ohmic contacts. Finally, antireflection coatings with reflectivity of less than 1% are applied to the both facets of devices.

Fig. 2 shows the fabricated laser array. The devices are numbered as No. 17, 18, 19 and 20.

The spectrum characteristics of the lasers' array are also measured. Fig. 3 shows the spectra of the SBW-DFB lasers' array at a same temperature of 25 °C. As shown in Fig. 3(a), all of the components of the SBW-DFB lasers' array behave single longitudinal mode property, and the lasing wavelengths are 1571.78 nm, 1575.53 nm, 1578.95 nm, 1583.17 nm respectively. And the SMSR of each component in the SBW-DFB lasers' array are 45.41 dB, 51.35 dB, 53.98 dB and 52.13 dB correspondingly.

We plot the lasing wavelengths' distribution of the SBW-DFB array in Fig. 3(b). As can be seen, the lasing wavelengths of the array's components behave a linear relationship, just as we have designed, with a maximum wavelength deviation of no larger than 0.3 nm, less than 1/10 of the wavelength spacing of our design. This test result demonstrates that our SBW-DFB can achieve a precise design of wavelengths' distribution for a suitable DFB laser array. Precise wavelength distribution proves that our theory is suitable for this SBW-DBR laser array, and it is suitable and low cost for precise WDM applications.

We plot the linewidth properties for laser No. 20 alone in Fig. 4. We get a best linewidth of 451 kHz at a current of 150 mA and 25 °C as shown in Fig. 4(a). The linewidth shows an excellent fit for Lorentz fitting. As we can see from Fig. 4(b), the linewidth goes down as the current increases. This is because linewidth is inversely proportional to lasing power while injection current is proportional to lasing power, which means linewidth should be inversely proportional to injection current. Maxium lasing linewidth is 1.93 MHz at 90 mA, which is still below 10 MHz. This demonstrates that the S bent introduced in our laser is good for wavelength distribution selection meanwhile cause almost no extra loss and maintain the linewidth property

The measured spectrum characteristics in different current injection for No. 20 of the SBW-DFB lasers' array are shown in Fig. 5. (a). The spectrum properties are measured at 25 °C water cooled condition. A clear single mode lasing property through the whole measured current from 80 mA to 150 mA can be seen and the center wavelength shifts from 1582.25 nm to 1585.75 nm, with a mode hop free tuning range larger than 3 nm with only current injection. We plot the lasing wavelength versus injection current for No. 20 of the SBW-DFB lasers' array at 25 °C water cooled condition in Fig. 5. (b), which shows a clear linear fitting property. The wavelength shifts every 0.05 nm per 1 mA. The tuning property caused by current injection is because the test is under water cooling condition, and the increase in current cause a corresponding temperature rise which makes the wavelength shift.

We measured the output power of the SBW-DFB lasers' array and show them in Fig. 6. All of the array's components behave good

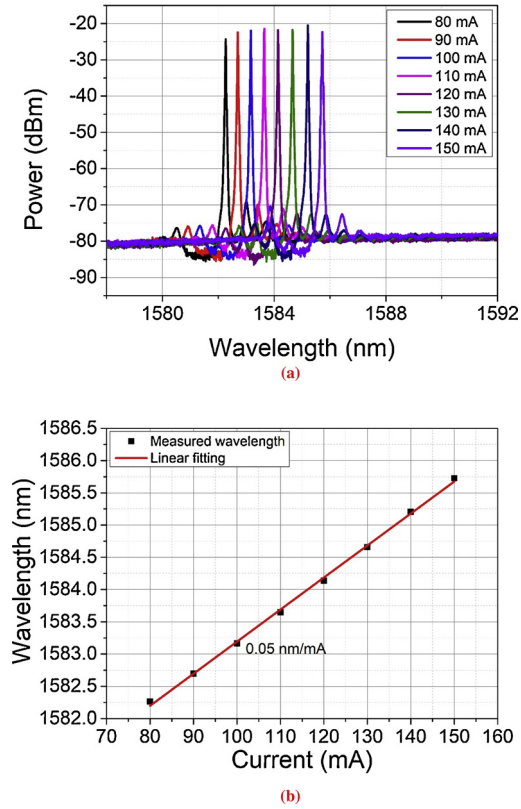


Fig. 5. (a) Measured spectrum characteristics in different current injection for No. 20 of the SBW-DFB lasers' array at 25 °C water cooled condition. (b) Lasing wavelength versus injection current for No. 20 of the SBW-DFB lasers' array at 25 °C water cooled condition.

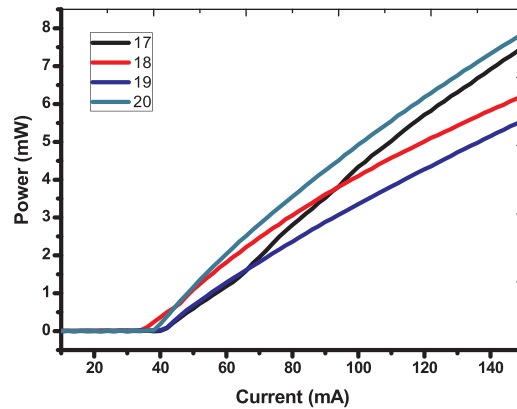


Fig. 6. Measured lasing power versus injection current for No. 17, 18, 19 and 20 of the SBW-DFB lasers' array.

lasing power property and the power are all above 5 mW. The threshold current is around 35 mA to 40 mA. The difference of the output of the power may come from the non-uniformity caused by the processing steps.

The most significant advantage of our proposed laser array structure is that, it can easily control the wavelengths' distribution of a certain laser array with high wavelength accuracy [17]. Our test result in Fig. 3 demonstrates the accuracy of wavelengths' distribution deviation less than 0.3 nm, and three out of the four lasers in the array have their lasing wavelengths' deviation less than 0.1 nm. This is very important when DFB laser arrays are used in WDM.

Another advantage of our SBW-DFB laser array is its simple processing steps. The only structure difference is the sampling periods, which differs from 5.095 μm , 5.367 μm , 5.648 μm and 5.972 μm . All the other parameters are the same. The results indicate that all the laser components of the SBW-DFB laser array operate in good single longitudinal mode with SMSRs higher than 45 dB. The fabrication steps are simple and compatible with the REC fabrication method, which means our SBW-DFB laser array is suitable for mass production and can be commercialized easily.

4. Conclusion

In this paper, a SBW-DFB laser array based on s-bent waveguide and sampled grating is designed and experimentally demonstrated. All of the components of the SBW-DFB laser array operate with high SMSR larger than 45 dB. The wavelengths distribution is controlled accurately utilizing the proposed method, achieving high wavelength precision of less than 0.3 nm wavelength deviation. Furthermore, the DFB lasers can be fabricated by the conventional holographic exposure and photolithography technique with much lower costs. Our proposed SBW-DFB laser array offers a promising way to fabricate multichannel DFB laser arrays for optical communications and photonic integrated circuits in the future.

Acknowledgements

This work is supported by National Science and Technology Major Project of China (2018YFB2200300); Frontier Science Key Program of the President of the Chinese Academy of Sciences (QYZDY-SSW-JSC006); National Natural Science Foundation of China (NSFC) (11874353, 61935009, 61934003, 61604151, 61674148, 61904179, 61727822, 11604328, 61805236); Dawn Talent Training Program of CIOMP.

References

- [1] T.-P. Lee, et al., Multiwavelength DFB laser array transmitters for ONTC reconfigurable optical network testbed, *J. Lightwave Technol.* 14 (6) (1996) 967–976.
- [2] Y. Sasahata, et al., Tunable DFB laser array integrated with Mach–Zehnder modulators for 44.6 Gb/s DQPSK transmitter, *IEEE J. Sel. Top. Quantum Electron.* 19 (4) (2013) p. 1501507.
- [3] S.-W. Ryu, S.-B. Kim, J.-S. Sim, J. Kim, Monolithic integration of a multiwavelength laser array associated with asymmetric sampled grating lasers, *IEEE J. Sel. Top. Quantum Electron.* 8 (6) (2002) 1358–1365.
- [4] T.-P. Lee, et al., Multiwavelength DFB laser array transmitters for ONTC reconfigurable optical network test bed, *J. Lightwave Technol.* 14 (6) (1996) 967–976.
- [5] H. Zhu, et al., The fabrication of eight-channel DFB laser array using sampled gratings, *IEEE Photonics Technol. Lett.* 22 (5) (2010) 353–355.
- [6] B. Zhang, Z. Wang, S. Brodbeck, et al., Zero-dimensional polariton laser in a subwavelength grating-based vertical microcavity, *Light Sci. Appl.* 3 (1) (2014) pp. e135:1–5.
- [7] C. Lu, X. Hu, K. Shi, et al., An actively ultrafast tunable giant slow-light effect in ultrathin nonlinear metasurfaces, *Light Sci. Appl.* 4 (6) (2015) pp. e302:1–9.
- [8] V.A. Fedotov, J. Wallauer, M. Walther, et al., Wavevector selective metasurfaces and tunnel vision filters, *Light Sci. Appl.* 4 (7) (2015) pp. e306:1–5.
- [9] J. Yang, Z. Wang, F. Wang, et al., Atomically thin optical lenses and gratings, *Light Sci. Appl.* 5 (3) (2016) pp. e16046:1–8.
- [10] D. Floess, J.Y. Chin, A. Kawatani, et al., Tunable and switchable polarization rotation with non-reciprocal plasmonic thin films at designated wavelengths, *Light Sci. Appl.* 4 (5) (2015) pp. e284:1–7.
- [11] L. Wang, X.W. Lin, W. Hu, et al., Broadband tunable liquid crystal terahertz waveplates driven with porous graphene electrodes, *Light Sci. Appl.* 4 (2) (2015) pp. e253:1–6.
- [12] T. Allsop, R. Arif, R. Neal, et al., Photonic gas sensors exploiting directly the optical properties of hybrid carbon nanotube localized surface plasmon structures, *Light Sci. Appl.* 5 (2) (2016) pp.e16036:1–8.
- [13] J. Qin, R.M. Silver, B.M. Barnes, et al., Deep subwavelength nanometric image reconstruction using Fourier domain optical normalization, *Light Sci. Appl.* 5 (2) (2016) pp. e16038:1–9.
- [14] T. Kjellberg, S. Nilsson, T. Klinga, B. Broberg, R. Schatz, Investigation on the spectral characteristics of DFB lasers with different grating configurations made by electron-beam lithography, *J. Lightwave Technol.* 11 (9) (1993) 1405–1415.
- [15] C. Vieu, et al., Electron beam lithography: resolution limits and applications, *Appl. Surf. Sci.* 164 (1/4) (2000) 111–117.
- [16] T. Kjellberg, R. Schatz, BThe effect of stitching errors on the spectral characteristics of DFB lasers fabricated using electron beam lithography, *J. Lightwave Technol.* 10 (9) (1992) 1256–1266.
- [17] Y.C. Shi, R. Liu, S.C. Liu, X.F. Chen, A low-cost and high-wavelength-precision fabrication method for multiwavelength DFB semiconductor laser array, *IEEE Photon. J.* 6 (3) (2014) 2400112.
- [18] Yuechun Shi, Simin Li, Xiangfei Chen, Lianyan Li, Jingsi Li, Tingting Zhang, Jilin Zheng, Yunshan Zhang, Song Tang, Lianping Hou, John H. Marsh, Bocang Qiu, High channel count and high precision channel spacing multi-wavelength laser array for future PICs, *Sci. Rep.* 4 (2014) 7377.
- [19] Yunshan Zhang, Yuechun Shi, Lianyan Li, Zhengpeng Zou, Jun Lu, Yinchao Du, Wenxuan Wang, Yating Zhou, Xin Chen, Jilin Zheng, Xiangfei Chen, Experimental demonstration of the distributed feedback semiconductor laser with S-Bent waveguide and sampled grating, *IEEE. Photon. J.* 9 (6) (2017) 1–12.
- [20] J. Li, et al., Experimental demonstration of distributed feedback semiconductor lasers based on reconstructionequivalent-chirp technology, *Opt. Exp.* 17 (7) (2009) 5240–5245.
- [21] Y.C. Shi, et al., Experimental demonstration of eight-wavelength distributed feedback semiconductor laser array using equivalent phase shift, *Opt. Lett.* 37 (16) (2012) 3315–3317.
- [22] J. Li, et al., B experimental demonstration of distributed feedback semiconductor lasers based on reconstructionequivalent-chirp technology, *Opt. Exp.* 17 (7) (2009) 5240–5245.